



## **DENSIFICATION BEHAVIOUR OF CAROB POWDER**

***Olaosebikan Layi Akangbe<sup>1</sup>, Radomír Adamovský<sup>1</sup>, Jiří Blahovec<sup>1</sup>,  
Kazimierz Rutkowski<sup>2</sup>***

*<sup>1</sup>Czech University of Life Sciences in Prague, <sup>2</sup>University of Agriculture in Krakow*

### ***Abstract***

The behaviour of carob (*Ceratonia siliqua* L.) powder relevant to its densification at low pressure was determined given different equipment aspect ratios (0.5, 1.0 and 1.5) and varying rates of deformation (5.5, 10 and 14.5 mm min<sup>-1</sup>). The effects of both parameters were examined through the analysis of variance and trends were fitted to observed mechanical responses using standard regression technique. Both aspect ratio and the time rate of deformation had highly significant effects on the material's response to load. Strain rate and specific power requirement were power functions of the equipment's aspect ratio, at all rates of deformation. These findings furnish insights on mechanical response in compressed food powders which are applicable in modelling related food handling and processing systems.

**Key words:** food powder, strain rate, aspect ratio, deformation

## **INTRODUCTION**

Available studies on mechanical behaviour of food materials under compressive loads describe their responses in terms of the loss of porosity (Faborode and O'Callaghan 1986, Raji and Favier 2004b). The expulsion of air and liquid essence constitutes a major component of this mechanism (Faborode 1989); particles within the material matrix are relocated, deformed and packed more closely. Densification may be applied to modify product forms or to achieve high

material and nutrient densities such as are important to their desirability, transport and storage (Akangbe and Herák 2017, Wójtowicz *et al.* 2015).

Although product depth is known to influence performance during densification (Divišová *et al.* 2014), it interacts with other system variables (Tumuluru 2015) and is influenced by material and process conditions (Karunanithy *et al.* 2012, Tumuluru 2014). This may also be perceived for strain when it varies with time due to the rate of effectuation of deformation (Gong *et al.* 2018). The influence of such interacting parameters, such as the depth of product charge and the equipment's characteristic dimension, on densification systems is seldom modelled. Available treatments are mostly with respect to force and deformation relationships (Herák *et al.* 2012). Although observed trends differ from material to material, it is possible to describe those behaviours with similar presentations (Nona *et al.* 2014). Fitting descriptions of the trends involved are important for describing densification systems. In this study, the effects of the rate of deformation and equipment aspect ratio on the densification of a highly functional food powder, namely carob were investigated and relationships described for important response parameters.

## MATERIALS AND METHODS

Carob (*Ceratonia siliqua* L.) powder, purchased in Czech Republic, was used for this study. The material had average particle size of 0.5 mm and initial bulk density of  $711.69 \pm 26.55 \text{ kg} \cdot \text{m}^{-3}$ .

A schematic view of the compression device is shown in figure 1. The device was comprised of cylindrical die, a base plug and a piston. The die had an internal bore diameter of 25 mm with wall thickness of 40 mm. The base plug is about 95 mm in diameter, stepped inwards diametrically at 25mm depth from its top, 35 mm from its circumference. The plug fits closely in the die sleeve. The solid piston provided is 200 mm long and 25mm in diameter. The compression device is mounted on the bed of a Tempos ZDM 50 universal test rig and loaded compressively through a flat topped, hemispherical disc.

Some volume measure of carob powder corresponding to an equipment aspect ratio was scooped, weighed and fed into the compression chamber. This sample was then gradually compressed a specified rate of deformation, up to a maximum compressive force of 25 kN, under laboratory conditions of 20°C. This corresponded to a maximum applied pressure of 50 MPa, at full load. Three rates of deformation (5.5, 10 and  $14.5 \text{ mm} \cdot \text{min}^{-1}$ ) and three equipment aspect ratios of 0.5, 1.0 and 1.5 were employed. An aspect is the depth of product in the compression chamber relative to the internal bore diameter of the compression vessel, which was 25 mm. There were nine treatments in all. Each test was repeated thrice and the total number of experimental runs was 27. This was a full

factorial experiment, fitted into a completely randomised design. Test data were logged electronically using the TiraTest software (TIRA GmbH, Schalkau, Germany). Samples were weighed using the Kern 440–35N (Kern & Sohn GmbH, Stuttgart, Germany) top-loading type weighing balance.

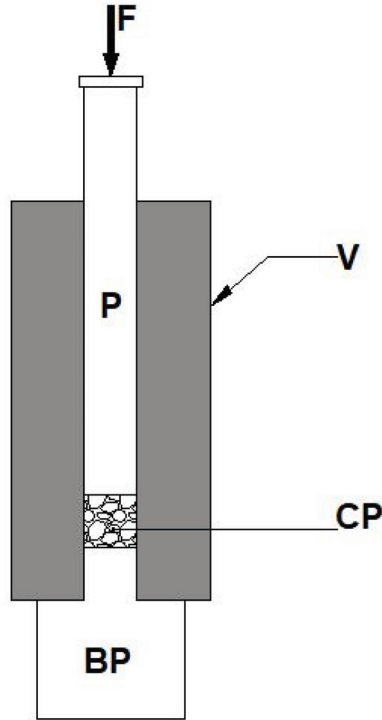


**Figure 1.** Schematic view of the product compression device showing the base plug, BP, compressed powder, CP, applied load, F, piston, P and cylindrical vessel, V.

Prior to densification, bulk density of the batch of carob powder used was determined as the ratio of the mass of a sample to the known free-fill volume (Mohsenin 1986). The highest value of deformation which was achieved for each crop at any given load was defined as  $\delta_c$  (mm). Where  $\delta_o$  (mm) is the initial height of pressed bulk seeds, the strain in the compressed material  $\epsilon$  (–) is given by Eq. 1

$$\epsilon = \frac{\delta_c}{\delta_o} \quad (1)$$

The initial volume of compressed material, ( $\text{mm}^3$ ) is given by Eq. 2

$$v = \frac{\pi D^2}{4} \times \delta_o \quad (2)$$

where,  $D$  (mm) is the inside diameter of the constraining cylindrical steel vessel.

Bulk density of the compressed material,  $\rho_c$  ( $\text{kg}\cdot\text{m}^{-3}$ ) was determined in relation to the mass ( $m_s$ ) and volume ( $v_c$ ) of the compressed product (Eq. 3).

$$\rho_c = \frac{m_s}{v_c} \quad (3)$$

The volume of the compressed product,  $v_c$  ( $\text{mm}^3$ ) may be calculated (Eq. 4) as follows:

$$v_c = \frac{\pi D^2}{4} \times \delta_f \quad (4)$$

where,  $\delta_f$  (mm) is the final height of the compressed material in the compression chamber.

The area beneath each force – deformation curve may be numerically computed using a trapezoidal rule (Eq. 5).

$$E = \sum_{n=0}^{n=i-1} \left[ \left( \frac{F_{n+1} + F_n}{2} \right) \times (\delta_{n+1} - \delta_n) \right] \quad (5)$$

This is the energy required for the indicated deformation of the compressed material,  $i$  being the number of subdivisions of the deformation axis or incremental deformation, logged by the test equipment (Akangbe and Herák 2017). For any deformation,  $\delta_n$  (mm),  $F_n$  (N) is the required force for that deformation. Expressed in terms of the volume of material compressed, specific energy demand,  $E_v$  ( $\text{J}\cdot\text{mm}^{-3}$ ) may be computed as shown in Eq. 6.

$$E_v = E/v \quad (6)$$

The time rate of the expenditure of this energy (specific power requirement,  $E'$ ) may be determined as shown in Eq. 7.

$$\dot{E} = E_v/t \quad (7)$$

A modulus,  $M_n$  may be described which includes both elastic and plastic components of deformation and is computed as the slope of the stress-strain curve (Eq. 8).

$$M_n = \left[ \frac{4 \times \delta_o}{\pi \times D^2} \left( \frac{F_{n+1} - F_n}{\delta_{n+1} - \delta_n} \right) \right]_{n=0}^{n=i-1} \quad (8)$$

Test data were analysed for variance using the completely randomised design model in Genstat. Treatment means were compared using Duncan’s multiple range test. All numerical computations and graphical plots were done using MS Excel.

## RESULTS AND DISCUSSION

The main effects of the rate of deformation and aspect ratio on the mechanical response parameters were highly significant ( $p < 0.001$ ), except for the effects of the rate of deformation on volume specific energy demand and deformation modulus, which were not significant (Table 1). The interactions of the rate of deformation and aspect ratio had significant effects on densification time, rate of strain and power, with no significant effects on other response variables.

**Table 1.** Effects of deformation rate and aspect ratio on response variables

Response parameter	Source of Variation		
	Deformation Rate, $D_R$	Aspect Ratio, $A_R$	$D_R \times A_R$
Deformation, $\delta$ (mm)	0.001**	0.001**	0.065 <sup>ns</sup>
Strain, $\epsilon$ (-)	0.001**	0.001**	0.144 <sup>ns</sup>
Strain rate, $\dot{\epsilon}$ ( $S^{-1}$ )	0.001**	0.001**	0.001**
Specific energy, $E_v$ ( $kJm^{-3}$ )	0.722 <sup>ns</sup>	0.001**	0.271 <sup>ns</sup>
Power, $E$ ( $kJm^{-3}S^{-1}$ )	0.001**	0.001**	0.001**
Deformation modulus, $M_n$ (MPa)	0.232 <sup>ns</sup>	0.001**	0.581 <sup>ns</sup>
Bulk density of compressed material, $\rho_c$ ( $kgm^{-3}$ )	0.001**	0.001**	0.265 <sup>ns</sup>
Gain in bulk density, $G_p$ (%)	0.001**	0.001**	0.265 <sup>ns</sup>

ns = not significant at the 5% level; \* = significant (at the 5% level); \*\* = highly significant (at the 1% level).

Force–deformation profiles of carob powder, compressed to a maximum load of 25 kN at 10 mm·min<sup>-1</sup>, are presented in Fig. 2. The trends are curvilinear and developed with incremental application of compressive load. Each curve indicates a high compressibility and improved packing with the onset and development of deformation (Raji and Favier 2004a). Similar amounts of deformation were achieved at rates of 10.0 and 14.5 mm·min<sup>-1</sup>. Deformation at 5.5 mm·min<sup>-1</sup> was significantly lower than these (Table 2). Deformation differed significantly

from one aspect ratio to another, being least at the lowest aspect ratio and increasing as aspect ratio increased (Table 3). Deformation rate correlated negatively with densification time and positively with aspect ratio. More time was required for densification at lower rates than at higher rates and densification time increased as the aspect ratio became larger. The most time was required for the largest aspect ratio at the lowest rate of deformation.

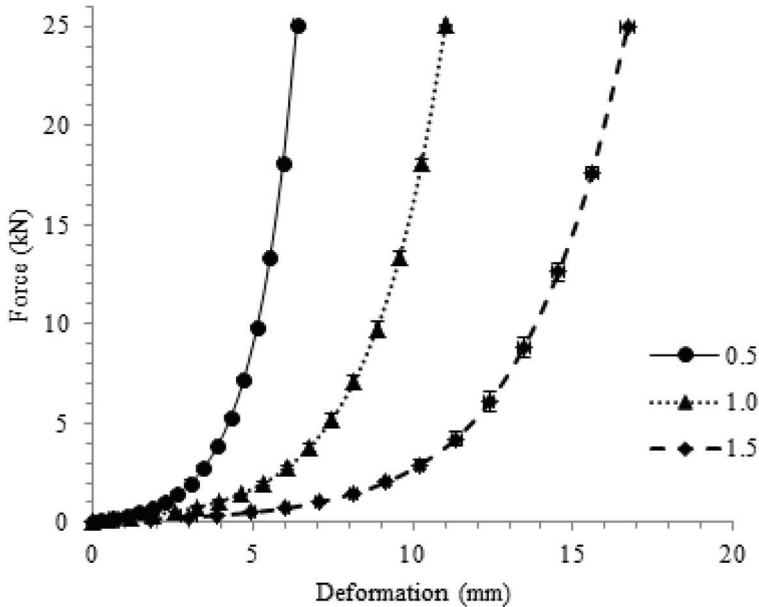


**Figure 2.** Force and deformation profiles of carob powder at aspect ratios of 0.5, 1.0 and 1.5, densified at a deformation rate of 10 mm min<sup>-1</sup>.

Strain induced at the rate of 5.5 mm min<sup>-1</sup> was lower than those induced at 10 and 14.5 mm min<sup>-1</sup> (Table 2). Also, the biggest amount of strain was associated with the smallest aspect ratio (Table 3).

Strain induced at an aspect ratio of 1.5 was higher than that induced at aspect ratio of 1.0 (Table 3) and could be attributed to the relative product depths. Not all strains are productive (Akangbe and Herak 2017). Within some regime, it has been shown (Mani *et al.* 2004) that a larger component of the applied pressure may be dissipated through rearrangement of particles within the material matrix. Hence, a significant amount of strain during the onset of deformation results from translocation of product particles, expulsion of air from the material matrix and the associated loss of void capacity.

**Table 2.** Main effects of the time rate of deformation on mechanical response parameters

Response Parameters	Deformation rate, $D_R$ ( $mm\ min^{-1}$ )		
	5.5	10.0	15.5
Deformation, $\delta$ (mm)	10.5 <sup>b</sup>	11.4 <sup>a</sup>	11.1 <sup>a</sup>
Strain, $\epsilon$ (-)	0.427 <sup>b</sup>	0.465 <sup>a</sup>	0.452 <sup>a</sup>
Strain rate, $\dot{\epsilon}$ ( $S^{-1}$ )	0.0045 <sup>c</sup>	0.0081 <sup>b</sup>	0.0117 <sup>a</sup>
Specific energy, $E_v$ ( $kJm^{-3}$ )	4.70 <sup>a</sup>	4.71 <sup>a</sup>	4.64 <sup>a</sup>
Power, $E$ ( $kJm^{-3}S^{-1}$ )	49.7 <sup>c</sup>	83.2 <sup>b</sup>	123.0 <sup>a</sup>
Deformation modulus, $M_n$ (MPa)	473.6 <sup>a</sup>	463.1 <sup>a</sup>	477.2 <sup>a</sup>
Bulk density of compressed material, $\rho_c$ ( $kgm^{-3}$ )	1246.0 <sup>b</sup>	1337.0 <sup>a</sup>	1307.0 <sup>a</sup>
Gain in bulk density, $G_p$ (%)	75.1 <sup>b</sup>	87.9 <sup>a</sup>	83.6 <sup>a</sup>

Mean values are compared row-wise. Similar alphabets indicate homogeneous subsets. Significant effects are valid at the 5% level of significance.

**Table 3.** Main effects of equipment aspect ratio on mechanical response parameters

Response Parameters	Aspect ratio, $A_R$ (-)		
	0.5	1.0	1.5
Deformation, $\delta$ (mm)	6.1 <sup>c</sup>	10.5 <sup>b</sup>	16.3 <sup>a</sup>
Strain, $\epsilon$ (-)	0.491 <sup>a</sup>	0.419 <sup>c</sup>	0.434 <sup>b</sup>
Strain rate, $\dot{\epsilon}$ ( $S^{-1}$ )	0.0132 <sup>a</sup>	0.0066 <sup>b</sup>	0.0044 <sup>c</sup>
Specific energy, $E_v$ ( $kJm^{-3}$ )	5.30 <sup>a</sup>	4.62 <sup>b</sup>	4.13 <sup>c</sup>
Power, $E$ ( $kJm^{-3}S^{-1}$ )	142.6 <sup>a</sup>	71.6 <sup>b</sup>	41.7 <sup>c</sup>
Deformation modulus, $M_n$ (MPa)	415.9 <sup>c</sup>	479.5 <sup>b</sup>	518.6 <sup>a</sup>
Bulk density of compressed material, $\rho_c$ ( $kgm^{-3}$ )	1443.0 <sup>a</sup>	1255.0 <sup>b</sup>	1193.0 <sup>c</sup>
Gain in bulk density, $G_p$ (%)	102.7 <sup>a</sup>	76.3 <sup>b</sup>	67.6 <sup>c</sup>

Mean values are compared row-wise. Similar alphabets indicate homogeneous subsets. Significant effects are valid at the 5% level of significance.

It's been argued (O'Dogherty 1989) that non-recoverable strain is a consistent portion of the maximum induced strain. Strain rate correlates positively with the rate of deformation and negatively with aspect ratio. The rate of strain at  $14.5\ mm\ min^{-1}$  was 44.6% and 161.4% above those occurring at  $10.0$  and  $5.5\ mm\ min^{-1}$ , respectively. The rate of strain at  $10.0\ mm\ min^{-1}$  was 80.7% more than that which occurred at  $5.5\ mm\ min^{-1}$ . With respect to aspect ratios, the rate of strain obtaining, given an equipment aspect ratio of 0.5 was 99.5% and 198.5% in ex-

cess of those obtaining at aspect ratios of 1.0 and 1.5, respectively; rate of strain, given an aspect ratio of 1.0, was 49.6% higher than that obtaining with an aspect ratio of 1.5. Whereas the former is in direct correlation to time, the later may be linked to the depth of product constituting the matrix through which the induced stress must be transmitted. This relationship is shown in figure 3. At each rate of deformation, strain rate fits (Table 4) as power functions of the equipment's aspect ratio – that is, the ratio of the compression height to the internal diameter of the compression vessel – and is of the form

$$\dot{\epsilon} = k r_a^n \tag{9}$$

where,  $\epsilon$  is the rate of strain ( $S^{-1}$ ),  $r_a$ , the aspect ratio (-), and  $k$  ( $S^{-1}$ ) and  $n$  are proportionality and exponential constants, respectively.

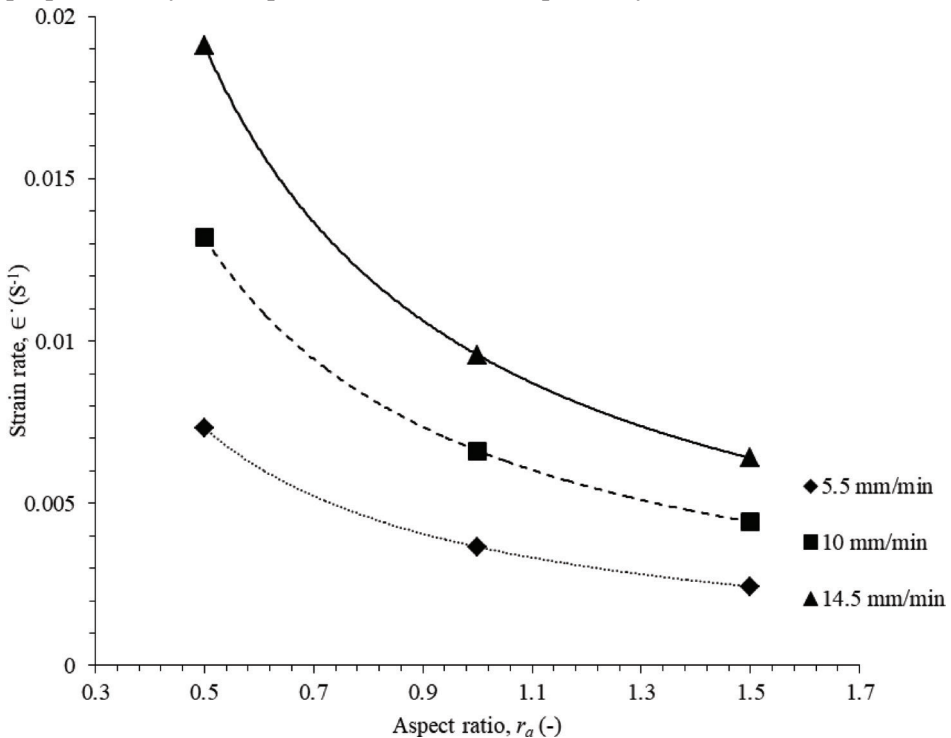


**Figure 3.** Effect of aspect ratio on the rate of strain at different rates of deformation.



**Table 4.** Estimates of function parameters fitted using the power rule

Deformation rate ( $S^{-1}$ )	Strain rate, $\epsilon$ $k$ ( $S^{-1}$ )			Specific power, $E$ ( $Jm^{-3} S^{-1}$ )		
	$K$ ( $S^{-1}$ )	$n$ (-)	$R^2$	$K$ ( $S^{-1}$ )	$n$ (-)	$R^2$
5.5	0.0037	-0.999	1.0	40129	-1.053	0.9680
10.0	0.0066	-0.993	1.0	66314	-1.088	0.9968
14.5	0.0096	-0.995	1.0	96502	-1.138	0.9967

Energy expended at the different aspect ratios differed significantly and was higher with smaller aspect ratios. A significant amount of this is stored in the material as plastic deformation (Kulig *et al.* 2015). With larger aspect ratios, energy demand per unit volume of material processed decreases (Table 3). This means that less power is required for at higher aspect ratios (Table 3). Power requirement correlated positively with the rate of deformation (Table 2) and negatively with aspect ratio (Table 3). As deformation rate increased, therefore, more energy was expended per unit time, for each volume of material densified. However, as aspect ratio decreased, more energy was expended per unit time for each volume of material densified. Volume specific rates of expenditure of energy were observed to be power functions of the aspect ratio (Eq. 10), at all rates of deformation (Figure 3), being of the form

$$\dot{E} = kr_a^n \quad (10)$$

where,  $E$  is the rate of expenditure of energy ( $Jm^{-3} S^{-1}$ ),  $r_a$ , the aspect ratio (-), and  $k$  ( $S^{-1}$ ) and  $n$  (-) are proportionality and exponential constants, respectively. The parameters of these equations are provided in Table 4. The parameter,  $k$  may be shown to be a rate dependent material property. The power law has been shown to describe the relationship between the ratio of in-die to relaxed material density and aspect ratio (O'Dogherty and Wheeler 1984).

Similar amounts of densification were achieved at 14.5 and 10.0  $mm \cdot min^{-1}$ ; less degree of densification was achieved at 5.5  $mm \cdot min^{-1}$ . Bulk density of the compressed material correlated negatively with aspect ratio. This effect is attributable to the effectiveness of the transfer of induced compressive stress along the longitudinal axis of the material matrix. Gain in bulk density was higher with smaller aspect ratios, and at higher rates of deformation (Tables 2 and 3). Only aspect ratios had effect on the deformation modulus (Table 3). This parameter is a measure of the material's resistance to strain.

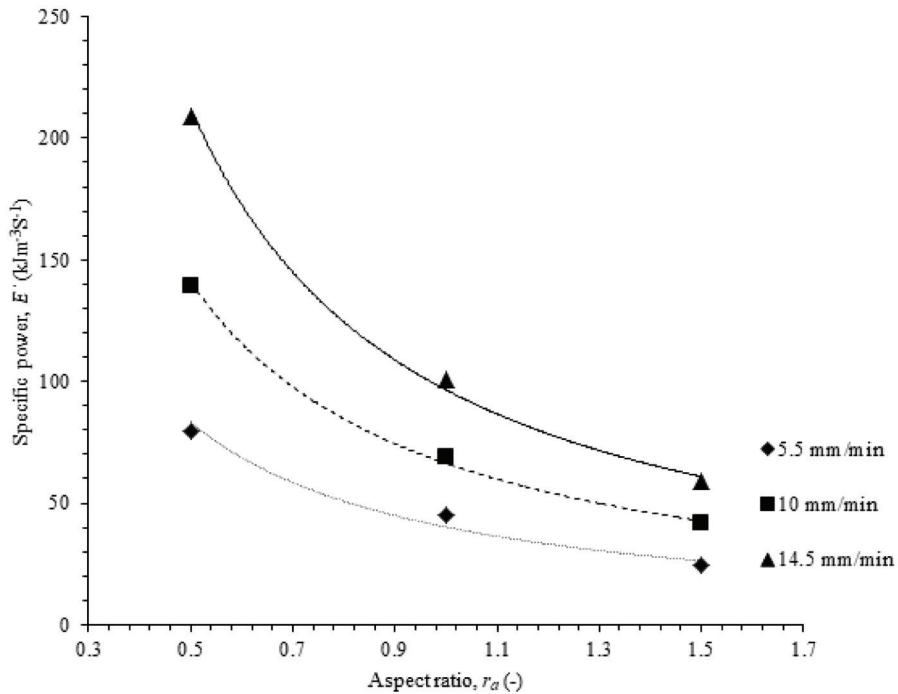


Figure 4. Effect of aspect ratio on specific power, at different rates of deformation

## CONCLUSIONS

In this study, the behaviour of carob powder under compressive load was investigated at different rates of deformation and aspect ratios. Both factors were found to influence mechanical response in the bulk material significantly. Whereas higher deformations may be associated with larger aspect ratios, associated strains do not necessarily translate completely to plastic deformation of the material. Specific energy requirement is lower and the rate of its expenditure better with larger aspect ratios. The rate of induction of strain and specific power are power functions of the aspect ratio. These observations are of particular relevance in equipment design.

## ACKNOWLEDGEMENT

This study was supported by the Integral Grant Agency of the Faculty of Engineering, Czech University of Life Sciences Prague, grant number: 2018: 31130/1312/3119.

## REFERENCES

- Akangbe, O. L., Herák, D. (2017). Mechanical behaviour of bulk seeds of some leguminous crops under compression loading. *Scientia Agriculturae Bohemica*, 48(4): 238–244.
- Divišová, M., Herák, D., Kabutey, A., Šleger, V., Sigalingging, R., Svatoňová, T. (2014). Deformation curve characteristics of rapeseeds and sunflower seeds under compression loading. *Scientia Agriculturae Bohemica*, 45(3): 180–186.
- Faborode, M. O. (1989). Moisture effects in the compaction of fibrous agricultural residues. *Biological Wastes*, 28(1), 61–71.
- Faborode, M. O., O’Callaghan, J. R. (1986). Theoretical analysis of the compression of fibrous agricultural materials. *Journal of Agricultural Engineering Research*, 35(3): 175–191.
- Gong, D., Nadolski, S., Sun, C., Klein, B., Kou, J. (2018). The effect of strain rate on particle breakage characteristics. *Powder Technology*, 339: 595–605.
- Herák, D., Kabutey, A., Sedláček, A., Gurdil, G. (2012). Mechanical behaviour of several layers of selected plant seeds under compression loading. *Research in Agricultural Engineering*, 58: 24–29.
- Karunanithy, C., Wang, Y., Muthukumarappan, K., Pugalendhi, S. (2012). Physiochemical Characterization of Briquettes Made from Different Feedstocks. *Biotechnology Research International*, 2012: 1–12.
- Kulig, R., Łysiak, G., Skonecki, S. (2015). Prediction of pelleting outcomes based on moisture versus strain hysteresis during the loading of individual pea seeds. *Biosystems Engineering*, 129: 226–236.
- Mani, S., Tabil, L. G., Sokhansanj, S. (2004). Evaluation of compaction equations applied to four biomass species. *Canadian Biosystems Engineering*, 46: 55–61.
- Mohsenin, N. N. (1986). *Physical properties of plant and animal materials. Vol I: structure, physical characteristics and mechanical properties* (2nd ed.). New York: Gordon and Breach Science Publishers.
- Nona, K. D., Lenaerts, B., Kayacan, E., Saeys, W. (2014). Bulk compression characteristics of straw and hay. *Biosystems Engineering*, 118: 194–202.
- O’Dogherty, M. J. (1989). A review of the mechanical behaviour of straw when compressed to high densities. *Journal of Agricultural Engineering Research*, 44: 241–265.
- O’Dogherty, M. J., Wheeler, J. A. (1984). Compression of straw to high densities in closed cylindrical dies. *Journal of Agricultural Engineering Research*, 29(1): 61–72.
- Raji, A. O., Favier, J. F. (2004a). Model for the deformation in agricultural and food particulate materials under bulk compressive loading using discrete element method . I : Theory, model development and validation. *Journal of Food Engineering*, 64: 359–371.

Raji, A. O., Favier, J. F. (2004b). Model for the deformation in agricultural and food particulate materials under bulk compressive loading using discrete element method. II: Compression of oilseeds. *Journal of Food Engineering*, 64(3): 373–380.

Tumuluru, J. S. (2014). Effect of process variables on the density and durability of the pellets made from high moisture corn stover. *Biosystems Engineering*, 119: 44–57.

Tumuluru, J. S. (2015). High moisture corn stover pelleting in a flat die pellet mill fitted with a 6 mm die: Physical properties and specific energy consumption. *Energy Science and Engineering*, 3(4): 327–341.

Wójtowicz, A., Mitrus, M., Oniszczyk, T., Mościcki, L., Kręcisz, M., Oniszczyk, A. (2015). Selected physical properties, texture and sensory characteristics of extruded breakfast cereals based on wholegrain wheat Flour. *Agriculture and Agricultural Science Procedia*, 7: 301–308.

Corresponding author: Olaosebikan Layi Akangbe  
prof. Ing. Radomír Adamovský, DrSc.  
prof. Ing. RNDr. Jiří Blahovec, DrSc.  
Czech University of Life Sciences in Prague  
Faculty of Engineering  
Kamycka 129, 16521 Praha 6 – Suchbát, Prague, Czech Republic  
Phone: +420 22438 3186  
e-mail: akangbe@tf.czu.cz

Prof. Eng. Kazimierz Rutkowski, PhD, DSc  
University of Agriculture in Krakow  
Faculty of Production and Power Engineering  
ul. Balicka 116b  
PL 30-149 Kraków  
Phone: +48 (12) 662 46 29  
e-mail: Kazimierz.Rutkowski@urk.edu.pl

Received: 30.11.2018

Accepted: 30.12.2018